

# UC Berkeley

## UC Berkeley Previously Published Works

### Title

Flexible Cobamide Metabolism in Clostridioides (Clostridium) difficile 630  $\Delta$ erm.

### Permalink

<https://escholarship.org/uc/item/0pf9s3vv>

### Journal

Journal of Bacteriology, 202(2)

### ISSN

0021-9193

### Authors

Shelton, Amanda N

Lyu, Xun

Taga, Michiko E

### Publication Date

2020-01-02

### DOI

10.1128/jb.00584-19

Peer reviewed



# Flexible Cobamide Metabolism in *Clostridioides (Clostridium) difficile* 630 $\Delta$ erm

Amanda N. Shelton,<sup>a</sup> Xun Lyu,<sup>b</sup> Michiko E. Taga<sup>a</sup>

<sup>a</sup>Department of Plant and Microbial Biology, University of California, Berkeley, Berkeley, California, USA

<sup>b</sup>Department of Molecular and Cell Biology, University of California, Berkeley, Berkeley, California, USA

**ABSTRACT** *Clostridioides (Clostridium) difficile* is an opportunistic pathogen known for its ability to colonize the human gut under conditions of dysbiosis. Several aspects of its carbon and amino acid metabolism have been investigated, but its cobamide (vitamin B<sub>12</sub> and related cofactors) metabolism remains largely unexplored. *C. difficile* has seven predicted cobamide-dependent pathways encoded in its genome in addition to a nearly complete cobamide biosynthesis pathway and a cobamide uptake system. To address the importance of cobamides to *C. difficile*, we studied *C. difficile* 630  $\Delta$ erm and mutant derivatives under cobamide-dependent conditions *in vitro*. Our results show that *C. difficile* can use a surprisingly diverse array of cobamides for methionine and deoxyribonucleotide synthesis and can use alternative metabolites or enzymes, respectively, to bypass these cobamide-dependent processes. *C. difficile* 630  $\Delta$ erm produces the cobamide pseudocobalamin when provided the early precursor 5-aminolevulinic acid or the late intermediate cobinamide (Cbi) and produces other cobamides if provided an alternative lower ligand. The ability of *C. difficile* 630  $\Delta$ erm to take up cobamides and Cbi at micromolar or lower concentrations requires the transporter BtuFCD. Genomic analysis revealed genetic variations in the *btuFCD* loci of different *C. difficile* strains, which may result in differences in the ability to take up cobamides and Cbi. These results together demonstrate that, like other aspects of its physiology, cobamide metabolism in *C. difficile* is versatile.

**IMPORTANCE** The ability of the opportunistic pathogen *Clostridioides difficile* to cause disease is closely linked to its propensity to adapt to conditions created by dysbiosis of the human gut microbiota. The cobamide (vitamin B<sub>12</sub>) metabolism of *C. difficile* has been underexplored, although it has seven metabolic pathways that are predicted to require cobamide-dependent enzymes. Here, we show that *C. difficile* cobamide metabolism is versatile, as it can use a surprisingly wide variety of cobamides and has alternative functions that can bypass some of its cobamide requirements. Furthermore, *C. difficile* does not synthesize cobamides *de novo* but produces them when given cobamide precursors. A better understanding of *C. difficile* cobamide metabolism may lead to new strategies to treat and prevent *C. difficile*-associated disease.

**KEYWORDS** 5-aminolevulinic acid, *Clostridioides difficile*, *Clostridium difficile*, cobalamin, cobamide, corrinoid enzymes, methionine synthase, nutrient transport, ribonucleotide reductase, vitamin B<sub>12</sub>

The human gut microbiota is a complex community composed of hundreds to thousands of species of bacteria, archaea, and eukaryotic microbes (1). Members of this community compete for nutrients such as carbon sources but also release metabolites that benefit other members. The exchange of B vitamins, particularly vitamin B<sub>12</sub>, is thought to be prevalent in many environments because most bacteria lack the ability to synthesize some of the cofactors that they require for enzyme catalysis (2–6) and instead must acquire them from other organisms (7). Such nutrient cross-feeding

**Citation** Shelton AN, Lyu X, Taga ME. 2020. Flexible cobamide metabolism in *Clostridioides (Clostridium) difficile* 630  $\Delta$ erm. *J Bacteriol* 202: e00584-19. <https://doi.org/10.1128/JB.00584-19>.

**Editor** Laurie E. Comstock, Brigham and Women's Hospital/Harvard Medical School

**Copyright** © 2020 American Society for Microbiology. All Rights Reserved.

Address correspondence to Michiko E. Taga, taga@berkeley.edu.

**Received** 13 September 2019

**Accepted** 26 October 2019

**Accepted manuscript posted online** 4 November 2019

**Published** 2 January 2020

interactions can influence bacterial metabolism in ways that can affect not only the microbiota but also host health (8, 9).

*Clostridioides (Clostridium) difficile* is a human intestinal pathogen that is among the most common causes of nosocomial infections, with nearly 300,000 health care-associated cases per year in the United States (10). *C. difficile* colonization of the gut is correlated with dysbiosis of the gut microbiota (11). Its abilities to germinate from spores, proliferate in the gut, and cause disease are impacted both positively and negatively by ecological and metabolic factors (12–14). The global alteration of the gut metabolome following antibiotic treatment is correlated with increased susceptibility to *C. difficile* infection, and recent work has linked changes in the relative abundance of specific metabolites to changes in the microbiome using model systems (11, 15–17). For example, succinate availability increases after disturbance of the microbiota, allowing *C. difficile* expansion in a mouse model (18). Additionally, specific commensal bacteria have been shown to produce compounds that stimulate *C. difficile* metabolism. In a bioassociation, *Bacteroides thetaiotaomicron* can break down host mucin and produce sialic acid, which can be used by *C. difficile* for expansion in the gut (19). *C. difficile* can also induce other members of the microbiota to produce indole, which is thought to create a more favorable environment for the pathogen by inhibiting competing microbes (20).

Some interactions with microbiota members have also been shown to be inhibitory to *C. difficile*. Coculturing with certain *Bifidobacterium* spp. on particular carbon sources reduces *C. difficile* toxin production relative to monoculture (21). While primary bile acids produced by the host promote *C. difficile* spore germination, *Clostridium scindens* and other 7 $\alpha$ -dehydroxylating *Clostridia* transform these compounds into secondary bile acids, which are inhibitory to *C. difficile* (22, 23). The latter example illustrates that compounds in the same class can have different effects on the disease state. Given the complexity of metabolic interactions in the mammalian gut, many additional microbial metabolites likely influence the ability of *C. difficile* to colonize and persist in the gut.

One class of metabolites that has not been explored for its ability to affect *C. difficile* growth and virulence is cobamides, the vitamin B<sub>12</sub> (also called cobalamin) family of cofactors. Cobamides are used in diverse metabolic pathways, including methionine synthesis, deoxyribonucleotide synthesis, acetogenesis, and some carbon catabolism pathways. These reactions are facilitated by fission of the Co-C bond to the cobamide upper ligand, which can be a 5'-deoxyadenosyl group for radical reactions, a methyl group for methyltransferase reactions, or a cyano group in the inactive vitamin form (24) (labeled "R" in Fig. 1A). Over 80% of all sequenced bacteria (25–27) and 80% of sequenced human gut bacteria (2, 28, 29) have one or more cobamide-dependent enzymes, suggesting that cobamides are widely used cofactors across microbial ecosystems. Strikingly, fewer than 40% of bacterial species are predicted to produce cobamides *de novo* (2, 25–28), and therefore, over half of the bacteria that use cobamides must acquire them from their environment. Cobamides vary in the structure of the lower ligand (Fig. 1A and B), and organisms studied to date are selective in which cobamides they can use (28, 30–37). Seven cobamides, in addition to the cobamide precursor cobinamide (Cbi) (Fig. 1C), have been detected in the human gut (38). In an environment with plentiful, diverse cobamides and cobamide precursors, a microbial species that requires a particular cobamide can either import that cobamide, synthesize it *de novo*, chemically remodel available cobamides to the preferred structure, or alter its need for the cobamide by using alternative pathways (8, 39).

The seven predicted cobamide-dependent enzymes encoded in the *C. difficile* genome are involved in methionine synthesis, nucleotide metabolism, and carbon metabolism (Fig. 2). When grown with amino acids and glucose as carbon and energy sources *in vitro*, *C. difficile* does not require cobalamin supplementation (40). However, in model infection systems, cobamide-dependent pathways may be important for virulence and growth. For example, access to ethanolamine catabolism may be important in modulating virulence, as deletion of EutA, the reactivating factor required for the activity of the cobamide-dependent ethanolamine ammonia lyase (EutBC), in *C. difficile*

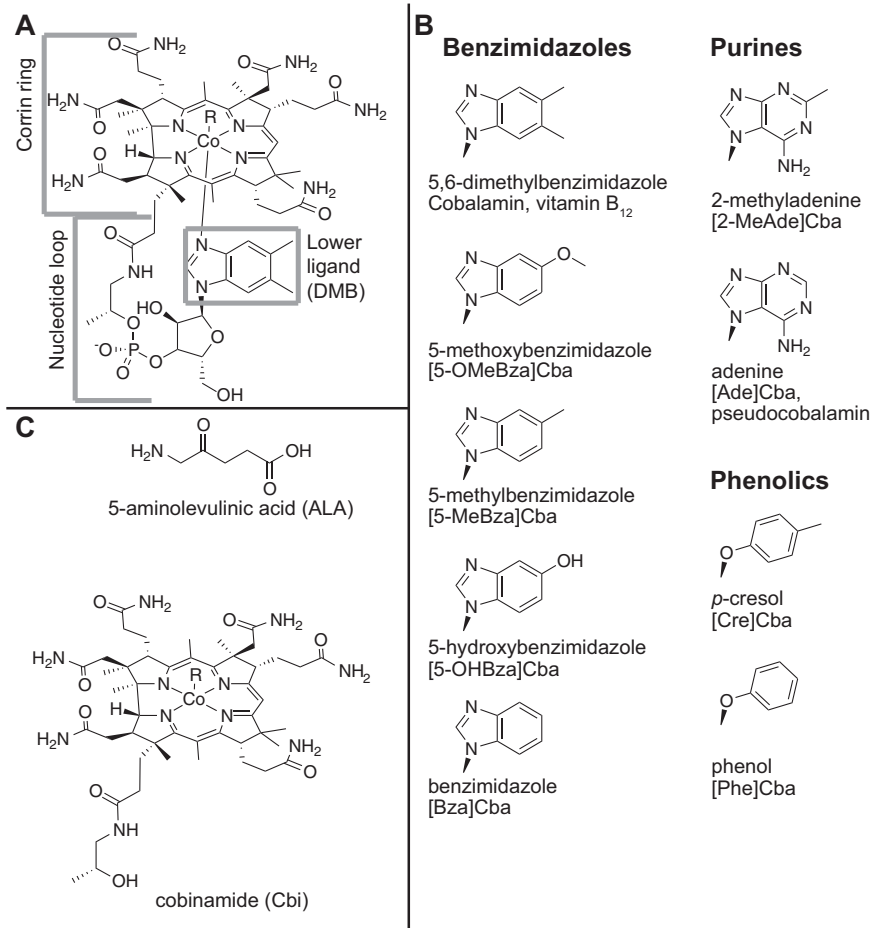


**FIG 1** Structures of cobamides and cobamide precursors. (A) Structure of cobalamin (B<sub>12</sub>). The corrin ring, nucleotide loop, and lower ligand are labeled. (B) Lower ligands of cobamides analyzed in this study, with the three structural classes labeled. The lower ligand name, abbreviation for the cobamide containing the lower ligand, and alternative names of the cobamide (when applicable) are indicated. (C) Cobamide precursors used in this study. R, upper ligand (-CN, -OH, -CH<sub>3</sub>, or 5'-deoxyadenosyl).

strain 630  $\Delta$ erm reduces the mean time to morbidity in a hamster model (41). Additionally, metabolic models and transcriptomics (42, 43) suggest that the cobamide-dependent Wood-Ljungdahl carbon fixation pathway is an important electron sink, and an experimental study suggests that it may be used for autotrophic growth by some *C. difficile* strains (44).

The observation that *C. difficile* can grow without added cobamides *in vitro* (40) suggests that it may not require cobamides under these conditions or that it can biosynthesize cobamides. However, all sequenced strains of *C. difficile* are missing HemA and HemL, the first two enzymes in the cobamide biosynthesis pathway required for the production of the precursor 5-aminolevulinic acid (ALA) (45) (Fig. 1C). Therefore, *C. difficile* is predicted to be able to produce a cobamide only when ALA is available, as has been observed in three other bacteria (25) (Fig. 2). In order to use cobamide-dependent pathways, we predict that *C. difficile* requires cobamides or precursors such as ALA from the gut. While ALA is an intermediate made in all tetrapyrrole-producing organisms, including the host, cobamides are produced by only some bacteria and archaea (46).

To address the importance of cobamides for *C. difficile* metabolism and to understand how *C. difficile* acquires cobamides, we examined *C. difficile* 630  $\Delta$ erm and mutant derivatives *in vitro* under cobamide-dependent conditions. We found that the bacterium can use a surprisingly diverse array of cobamides for growth requiring cobamide-dependent methionine and deoxyribonucleotide synthesis and can use alternative nutrient sources or

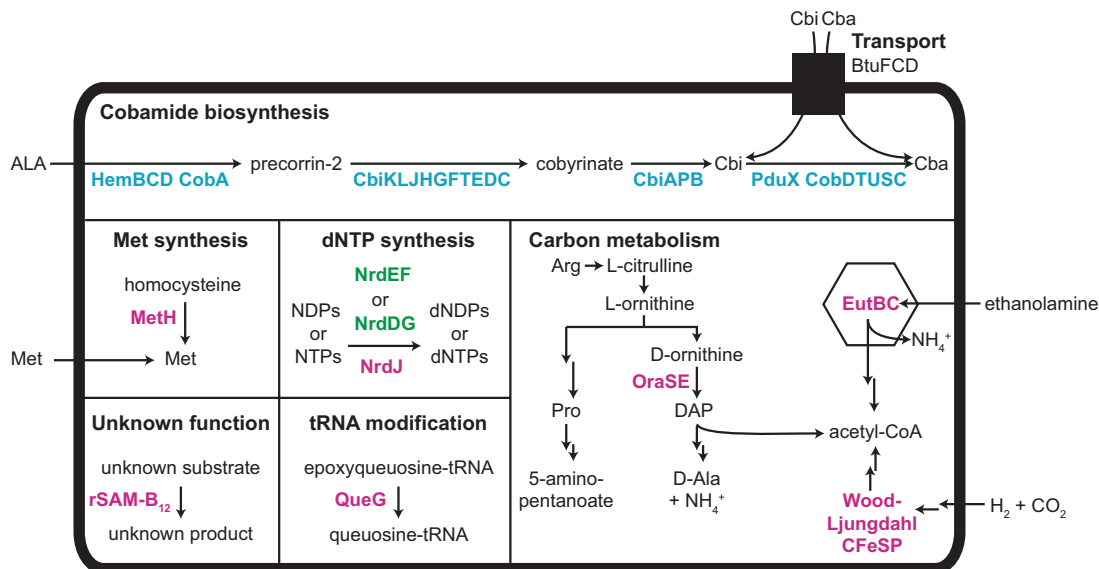


**FIG 2** Predicted cobamide biosynthetic and cobamide-dependent pathways in *C. difficile* 630  $\Delta$ erm. The enzymes of the cobamide biosynthesis pathway are shown in blue text, homologs of cobalamin-dependent enzymes are in magenta text, cobalamin-independent isozymes are in green text, and the transporter BtuFCD is shown as a black rectangle. Abbreviations: Cba, cobamide; Cbi, cobinamide; ALA, 5-aminolevulinic acid; rSAM, radical S-adenosylmethionine; NDPs, ribonucleoside diphosphates; NTPs, ribonucleoside triphosphates; dNDPs, deoxyribonucleoside diphosphates; dNTPs, deoxyribonucleoside triphosphates; DAP, 2,4-diaminopentanoate. Standard amino acid abbreviations are used. Enzymes: Meth, cobalamin-dependent methionine synthase; NrdEF, cobalamin-independent, aerobic (oxygen-requiring) (class I) ribonucleotide reductase (RNR); NrdDG, cobalamin-independent, anaerobic (oxygen-sensitive) (class III) RNR; NrdJ, cobalamin-dependent (class II) RNR; QueG, epoxyqueuosine reductase; EutBC, ethanolamine ammonia lyase; CFESF, corrinoid iron-sulfur protein; OraSE, D-ornithine 4,5-aminomutase.

enzymes to fulfill its metabolic needs. In addition to importing and using a variety of cobamides, when provided with ALA or the late intermediate Cbi, *C. difficile* 630  $\Delta$ erm can produce the cobamide pseudocobalamin and can produce other cobamides if provided an alternative lower ligand. Together, these results show that *C. difficile* is versatile in its cobamide metabolism.

## RESULTS

***C. difficile* requires methionine or a cobamide for growth.** To investigate cobamide-dependent metabolism in the model *C. difficile* strain 630  $\Delta$ erm, we sought to culture the organism under conditions that require specific cobamide-dependent enzymes. The *C. difficile* genome encodes the cobalamin-dependent methionine synthase MetH but does not contain the cobalamin-independent alternative enzyme MetE. The absence of a complete cobamide biosynthesis pathway suggests that *C. difficile* requires either methionine or a cobamide in its growth medium. Previously, methionine was classified as a “growth-enhancing,” but not essential, amino acid in a medium containing cyanocobalamin (vitamin B<sub>12</sub>) for seven of eight strains tested (40, 47). To test whether *C. difficile* can use cobamides for methionine synthesis and to identify the specific cobamides that support its MetH-dependent growth, we cultured *C. difficile* in a defined medium lacking methionine with a range of concentrations of cyanocobalamin, Cbi, and eight other cyanylated cobamides that we purified. *C. difficile* was unable to grow in this medium without cobamide or methionine addition (Fig. 3A), suggesting that, as predicted, it cannot produce cobamides *de novo* to support the activity of MetH. Remarkably, unlike other bacteria that have been reported to use a limited number of cobamides for methionine synthase activity (28, 48, 49), all of the cobamides and Cbi were able to confer high growth yields to *C. difficile* at concentrations as low as 1 nM (Fig. 3A). Methionine addition also supported growth, although higher concentrations were required than for cobamides (Fig. 3B). We also observed robust growth with the addition of ALA (Fig. 3C).

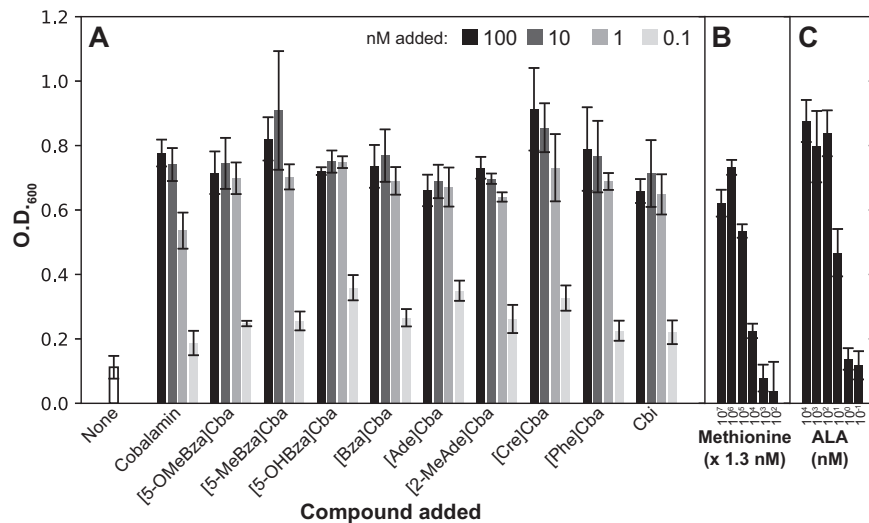


**FIG 3** *C. difficile* can use a broad range of cobamides for Meth-dependent growth. The OD<sub>600</sub>s of *C. difficile* 630  $\Delta$ erm cultures grown to saturation (22.5 h) in CDDMK plus glucose without methionine and with the addition of cobamides or Cbi (A), methionine (B), and ALA (C) are shown. The means and standard deviations of data from four biological replicates are shown in the bars and error bars, respectively.

***C. difficile* growth with the ribonucleotide reductase NrdJ requires a more restricted set of cobamides.** *C. difficile* genomes encode homologs of the cobalamin-dependent (class II) ribonucleotide reductase (RNR) (*nrdJ* [CDIF630erm\_RS07280]) as well as two cobalamin-independent RNRs: an oxygen-dependent (class I) RNR (encoded by *nrdE* [CDIF630erm\_RS16325] and *nrdF* [CDIF630erm\_RS16320]) and an oxygen-sensitive (class III) RNR (*nrdD* [CDIF630erm\_RS00990] and *nrdG* [CDIF630erm\_RS00995]). In principle, any of these three isozymes could be used for deoxyribonucleotide synthesis from ribonucleotides, although under anaerobic conditions, only the class II and class III RNRs are expected to function. Cobamide addition is not required for anaerobic growth of the parent strain *C. difficile* 630  $\Delta$ erm  $\Delta$ pyrE in a Casamino Acids medium (*Clostridium difficile* defined medium [CDDM]) with glucose, and the addition of cobamides or cobamide precursors did not affect the growth yield (see Fig. S1 in the supplemental material), suggesting that the class III RNR NrdDG is functional under these conditions. To test whether the class II RNR NrdJ is functional, we deleted the *nrdD* and *nrdG* genes while providing exogenous cobalamin, using the allelic exchange system in a  $\Delta$ pyrE background (50). This strain could grow only with cobalamin addition, suggesting that NrdJ is functional and NrdEF is not under these growth conditions (Fig. 4A). To determine which cobamides it requires, the  $\Delta$ nrdDG strain was grown with the same cobamides and precursors as those in Fig. 3. In contrast to growth under MethH-requiring conditions, the NrdJ-dependent conditions showed more selectivity in which cobamides supported growth (Fig. 4A), as expected based on studies with other class II RNRs (33, 36, 51, 52). There was little growth with [Cre]Cba, [Phe]Cba, and [5-OH-Bza]Cba (see Fig. 1B for cobamide abbreviations) (Fig. 4A). The addition of ALA also supported NrdJ-dependent growth (Fig. 4B).

***C. difficile* produces pseudocobalamin from the precursor ALA via the *cbi* genes.** The observation that *C. difficile* could grow under cobamide-dependent conditions with ALA or Cbi (Fig. 3A and C and Fig. 4) suggests that it can produce a cobamide from these precursors using the cobamide biosynthetic genes encoded in its genome (25). To test this prediction, the corrinoid fraction, which includes cobamides and late cobamide precursors, including Cbi, was extracted from the cell pellets of *C. difficile* 630  $\Delta$ erm grown with either ALA or Cbi. Consistent with our predictions, high-performance liquid chromatography (HPLC) analysis of the extracted corrinoids showed that *C. difficile* produced a cobamide only when ALA or Cbi was added (Fig. 5A). We con-

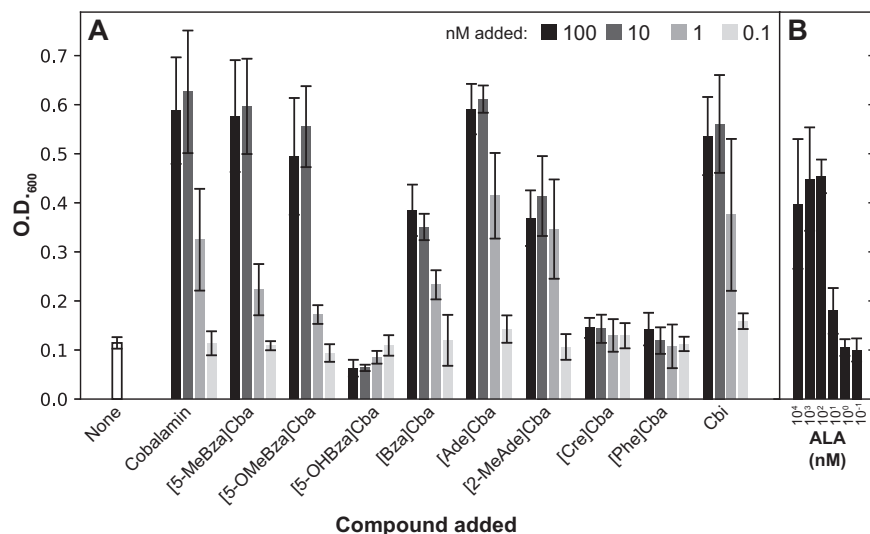


**FIG 4** *C. difficile* is selective in which cobamides it can use for NrdJ-dependent growth. The OD<sub>600</sub>s of *C. difficile* 630  $\Delta$ erm  $\Delta$ pyrE  $\Delta$ nrdDG cultures grown to saturation (22.5 h) in CDDM with added uracil and glucose are shown for cobamides and Cbi (A) and ALA (B) added. The means and standard deviations of data from three biological replicates are shown in the bars and error bars, respectively.

structured a strain lacking the corrin ring biosynthesis genes *cbiKJLJHGFTEDC*, and, as predicted, corrinoid analysis of this strain demonstrated that these genes are necessary for cobamide synthesis from ALA but not Cbi (Fig. 5A). Because *C. difficile* lacks all known genes for the biosynthesis of benzimidazoles and the attachment of phenolic lower ligands, it is predicted to be incapable of producing benzimidazolyl or phenolyl cobamides but may produce a purinyl cobamide (49, 53–59). Indeed, the major cobamide present in *C. difficile* corrinoid extracts coeluted with the purinyl cobamide pseudocobalamin (Fig. 5A). The UV-visible (UV-Vis) spectrum of the major cobamide was consistent with a pseudocobalamin standard (Fig. S2C). Mass spectrometry analysis verified that the major cobamide extracted from cultures grown with ALA is pseudocobalamin (Fig. S2A and B).

#### ***C. difficile* can perform guided biosynthesis but does not remodel cobamides.**

Some bacteria can perform guided biosynthesis, a process in which an exogenously provided, nonnative lower ligand base is incorporated into a cobamide (32, 36, 48, 60, 61). To test if *C. difficile* is capable of guided biosynthesis to produce cobamides other than its native pseudocobalamin, either dimethylbenzimidazole (DMB) (the lower ligand of cobalamin) (Fig. 1A) or a related compound, benzimidazole (Bza) (Fig. 1B), was added to cultures containing either ALA or Cbi. Analysis of corrinoid extracts showed that *C. difficile* could attach either of these exogenous lower ligands to form cobalamin and [Bza]Cba, respectively, with both precursors (Fig. 5B). A small amount of pseudocobalamin was also recovered in cultures containing Cbi with Bza (Fig. 5B).

Some bacteria and archaea are able to remodel cobamides by removing the lower ligand and nucleotide loop with the amidohydrolase enzyme CbiZ and rebuilding the cobamide with a different lower ligand (31, 62–64). We were unable to identify a *cbiZ* homolog in the *C. difficile* genome, and accordingly, we did not observe evidence of remodeling: when cobalamin, [2-MeAde]Cba, or [Cre]Cba was provided to *C. difficile*, the same cobamides were recovered from the cells (Fig. 6A).

***C. difficile* requires *btuFCD* for efficient uptake of cobamides and Cbi.** The presence of cobamides in the cellular fraction of cultures grown with either Cbi or a cobamide at nanomolar concentrations (Fig. 5 and Fig. 6A) suggested that *C. difficile* takes up Cbi and cobamides via an active transporter. We identified a candidate cobalamin uptake operon (*btuFCD*) downstream of a sequence annotated as a cobalamin riboswitch, suggesting that these genes function in corrinoid import, and con-

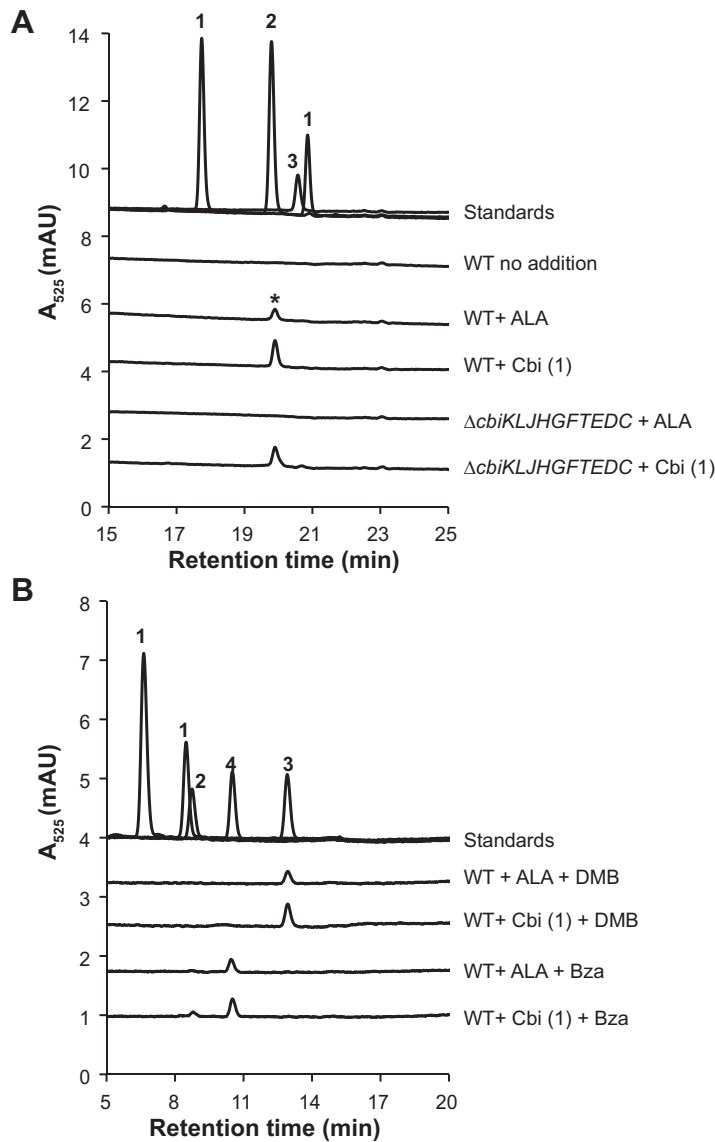


**FIG 5** HPLC analysis of corrinoid extracts from *C. difficile* cultures. (A) HPLC analysis of corrinoid extracts from cell pellets of *C. difficile* 630  $\Delta$ *erm* (wild type [WT]) and 630  $\Delta$ *erm*  $\Delta$ *pyrE*  $\Delta$ *cbiKJHGFTEDC* grown to saturation in CDDM with glucose with either 100 nM ALA or 10 nM dicyanocobinamide (Cbi) added. An asterisk indicates the corrinoid peak validated by mass spectrometry (see Fig. S2 in the supplemental material). (B) HPLC analysis of corrinoid extracts of *C. difficile* 630  $\Delta$ *erm* grown with either 100 nM ALA or 10 nM Cbi and 100 nM lower ligand base DMB or Bza. An Agilent Eclipse Plus C<sub>18</sub> column and an Agilent Zorbax SB-Aq column were used to separate corrinoid extractions in panels A and B, respectively. Cbi (compound 1), pseudocobalamin (compound 2), cobalamin (compound 3), and [Bza]Cba (compound 4) are shown as standards. mAU, milli-absorbance units.

structed a deletion mutant of this operon (27, 28, 65–70). No corrinoids could be detected in the cellular fraction of the  $\Delta$ *btuFCD* mutant grown with 10 nM Cbi or cobalamin (Fig. 6A). In contrast, ALA uptake is apparently unaffected in the  $\Delta$ *btuFCD* mutant, as pseudocobalamin can be recovered from the cellular fraction when ALA is provided (Fig. 6A). Furthermore, the  $\Delta$ *btuFCD* mutant grew poorly in methionine-free medium even when Cbi or cobalamin was added at concentrations that were 10<sup>3</sup>- to 10<sup>4</sup>-fold higher than what is required for the growth of the parental strain (Fig. 6B). The ability of methionine or ALA to support growth remained unaffected by the  $\Delta$ *btuFCD* mutation (Fig. 6B). Interestingly, genomic analysis identified strains of *C. difficile* that contain a *tlpB* transposon insertion in *btuC*, likely rendering the BtuFCD transporter



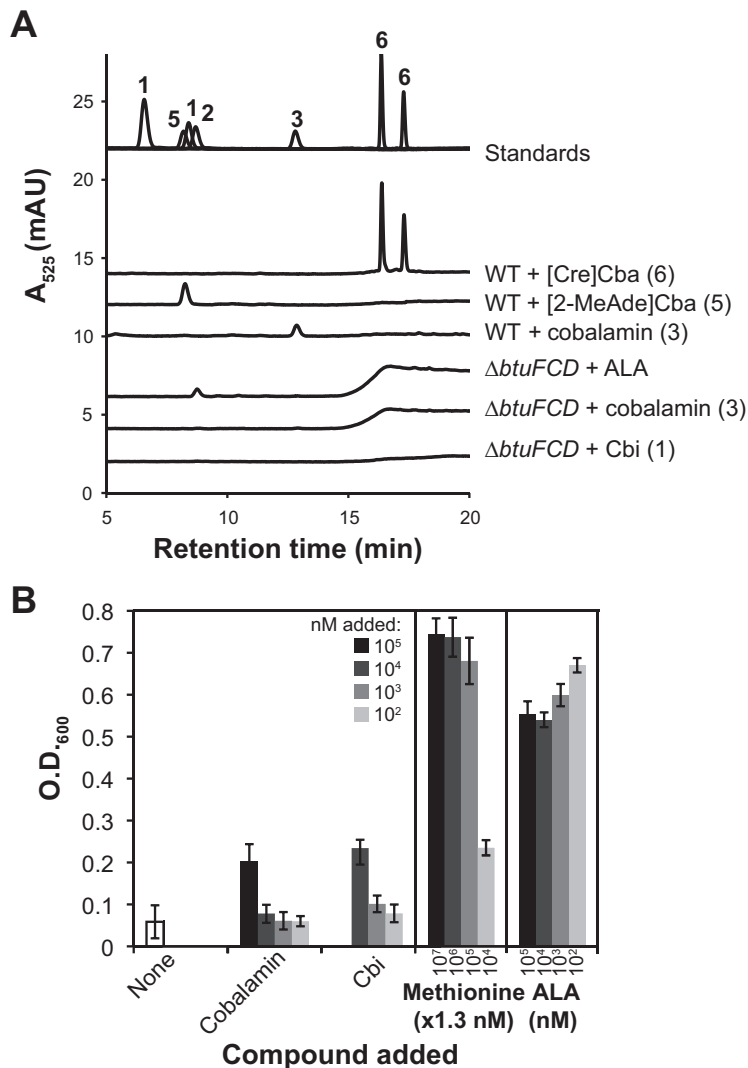


**FIG 6** The *C. difficile*  $\Delta btuFCD$  mutant is impaired in cobamide and Cbi uptake. (A) HPLC analysis of corrinoid extracts from cell pellets of *C. difficile* 630  $\Delta erm$  (WT) and *C. difficile* 630  $\Delta erm \Delta pyrE \Delta btuFCD$  grown with 10 nM cobamides or 100 nM ALA. Cbi (compound 1), pseudocobalamin (compound 2), cobalamin (compound 3), [2-MeAde]Cba (compound 5), and [Cre]Cba (compound 6) are shown as standards. mAU, milli-absorbance units. (B) Growth of *C. difficile* 630  $\Delta erm \Delta pyrE \Delta btuFCD$  under MethH-dependent conditions. The OD<sub>600</sub>s of saturated cultures (23.5 h) in CDDMK without methionine plus glucose and uracil are plotted as a function of the amount of the compound added. Bars and error bars are the means and standard deviations of data from three biological replicates.

nonfunctional (Fig. 7A) (71). Of the genomes analyzed, the *tlpB* insertion in this locus appears to be restricted to strains in the PCR ribotype 027 (RT027) clade, including the hypervirulent strain R20291, based on a multilocus sequence typing (MLST) tree of *C. difficile* strains (Fig. 7B, red labels). This observation suggests that unlike strain 630  $\Delta erm$  examined in this study, members of the RT027 clade may be unable to take up cobamides and Cbi efficiently.

## DISCUSSION

The potential of *C. difficile* to cause disease is closely linked to its ability to fill ecological niches made available by gut microbiota dysbiosis (13), using a suite of metabolic pathways to make use of newly available nutrient sources. *C. difficile* has an unusually high number of cobamide-dependent pathways encoded in its genome (25), but their functions have been underexplored. Here, we show that *C. difficile* is able to use many cobamides and cobamide precursors in two of its seven cobamide-

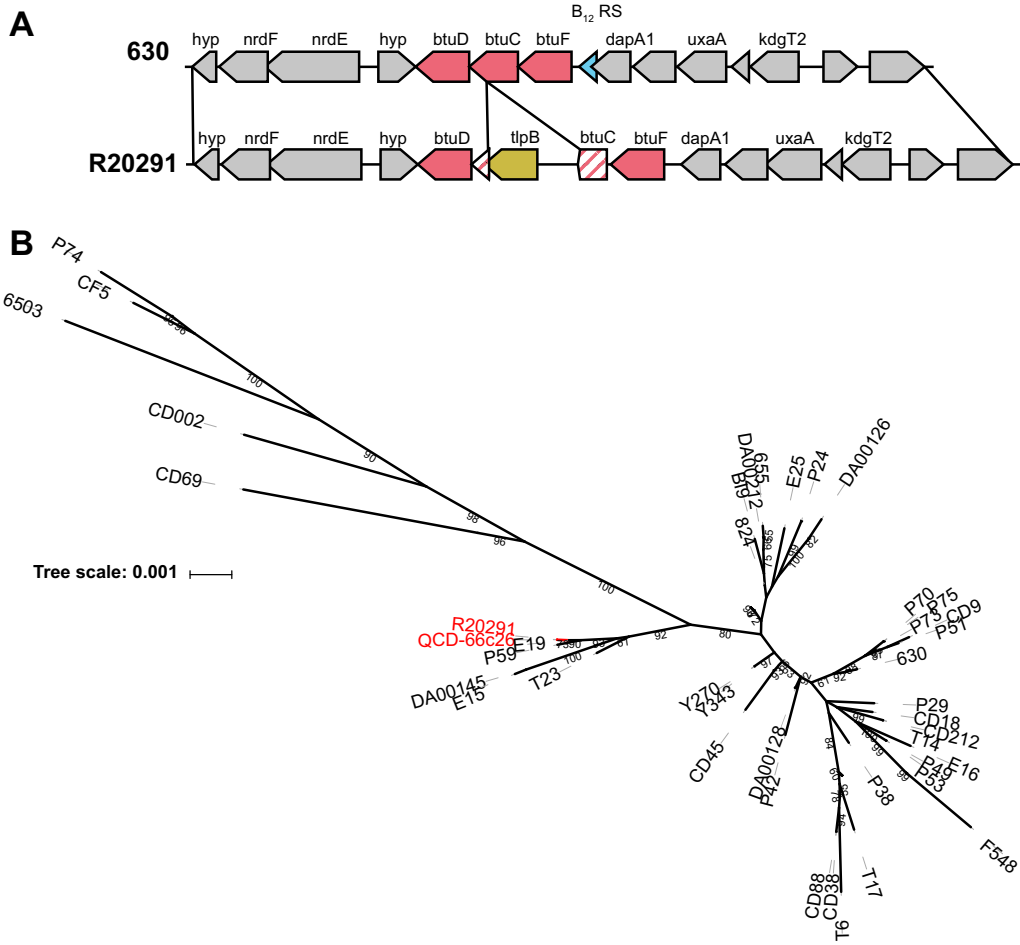


**FIG 7** Distribution of the *tlpB* transposon insertion in *btuC* in *C. difficile* strains. (A) Gene neighborhood diagram of strain 630, which lacks the *tlpB* insertion, and strain R20291, which has a *tlpB* insertion in *btuC* (shown in yellow). The *btuC* pseudogene is indicated by pink stripes. Gene names are shown. (B) Maximum likelihood multilocus sequence typing (MLST) tree of 79 *C. difficile* strains labeled with their strain designation. Branch labels are support values from 100 bootstraps. Genomes with the *tlpB* insertion in *btuC* are labeled in red, and those without the *tlpB* insertion in *btuFCD* are in black. Clades with average branch lengths of <0.0001 substitution per site have been collapsed, and bootstrap values of <50 have been removed to improve readability.

dependent pathways. The promiscuous use of cobamides and the ability to bypass these cobamide-dependent pathways highlight the metabolic flexibility of *C. difficile*.

The cobalamin-dependent methionine synthase MetH is the most abundant cobamide-dependent enzyme encoded in bacterial genomes (25) and is found in numerous organisms in all three domains of life, including humans (24). Compared to the majority of other MetH homologs that have been studied, our MetH-dependent growth results indicate that the *C. difficile* MetH homolog is unusually promiscuous in its cobamide selectivity. For example, several eukaryotic algae grew robustly under MetH-dependent conditions with cobalamin but did not grow with pseudocobalamin at the same concentrations (33). The human gut commensal bacterium *Bacteroides thetaiotaomicron* could use benzimidazolyl and purinyl cobamides for MetH-dependent growth but could not use phenolyl cobamides (28). An example of MetH selectivity *in vitro* was in *Spirulina platensis*, where the purified enzyme bound its native cobamide, pseudocobalamin, with a higher affinity than for cobalamin (72). An exception to this observed selectivity is another gut pathogen, *Salmonella enterica*, which can use its native cobamide, pseudocobalamin, in addition to cobalamin, [Phe]Cba, and [Cre]Cba, for MetH-dependent growth, although other cobamides were not tested (48, 49). The versatility of *C. difficile*'s cobamide use is notable given the diversity of cobamides that have been detected in the gut (38).

In contrast to MetH, our growth experiments indicate that the selectivity of *C. difficile* NrdJ is more similar to those of other organisms that rely on NrdJ for growth. For example, *Sinorhizobium meliloti* was unable to grow with [Cre]Cba and grew poorly with pseudocobalamin relative to its native cobamide, cobalamin (36); *Lactobacillus leichmannii* could use only benzimidazolyl or purinyl cobamides (51); and *Euglena gracilis* grew well with cobalamin and [Bza]Cba and poorly with pseudocobalamin, [5-OHBza]Cba, and [Cre]Cba (33, 52). Unlike MetH, the NrdJ enzyme requires cobamides that can adopt the “base-on” configuration in which the lower ligand base is coordinated to the cobalt ion throughout the catalytic cycle (24). Phenolyl cobamides are unable to adopt the base-on configuration, so their inability to support growth under NrdJ-dependent conditions was expected. *C. difficile* 630  $\Delta$ erm also contains an active class III cobamide-independent RNR, NrdDG, which may be an important strategy to maintain deoxyribonucleotide synthesis when cobamides are scarce. However, in other species, under certain conditions, the class II RNR provides an advantage over other RNR classes, such as during oxidative stress (73), although the conditions where NrdJ would provide an advantage for *C. difficile* have yet to be uncovered.

Seven different cobamides and the precursor Cbi have been detected in human feces (38). In stool samples of individuals not taking cobalamin supplements, the average amount of total corrinoid present is approximately 1,300 ng per g of feces, roughly equivalent to 1  $\mu$ M (38). Cbi is found at tens of nanograms per gram (38). Growth experiments under MetH- and NrdJ-dependent conditions showed that *C. difficile* 630  $\Delta$ erm reached maximum growth yields with as little as 1 nM cobamide or Cbi (Fig. 3 and 4). Based on the absence of corrinoids in the cellular fraction of a 630  $\Delta$ erm  $\Delta$ pyrE  $\Delta$ btuFCD strain (Fig. 6), we infer that strains with an insertion in *btuC* (Fig. 7), including the hypervirulent R20291 and CD196 strains (71), would require cobamides or Cbi at extracellular concentrations higher than 100  $\mu$ M if relying on cobamide-dependent enzymes. This suggests that these strains may not be able to use the cobamides or Cbi present in the gut.

Our results show that not only is *C. difficile* able to use multiple cobamides to support its metabolism, but it can also use the early precursor ALA to produce pseudocobalamin. The ability to use ALA to produce a cobamide, and, thus, not strictly rely on cobamide or Cbi uptake, could be important to strains with a transposon insertion in the *btuC* gene (Fig. 7) (70, 74). ALA concentrations in the human gut have not been reported. However, we speculate that, similar to cobamides and Cbi, ALA and possibly other early cobamide precursors could be provided by other members of the microbiota. Alternatively, ALA could be provided by the host either through the diet or via the biosynthesis of heme, which also uses ALA as a precursor. Members of the commensal gut microbiota have been reported to be able to salvage ALA (25), suggesting that ALA could be available in the gut.

*C. difficile* is also able to incorporate nonnative lower ligands to form benzimidazolyl cobamides (guided biosynthesis). Free benzimidazole bases have been found in animal gastrointestinal tracts, such as in rumen fluid and termite guts (75), but benzimidazole levels in the human gut have not been measured. The cobamides used by *C. difficile* could therefore also vary with the presence of different benzimidazole-producing organisms in the microbiota. Our results show that pseudocobalamin and most benzimidazolyl cobamides support the growth of *C. difficile* equally for the two pathways that we investigated in this study, but the cobamide preferences of the other five cobamide-dependent pathways have not been investigated.

We have identified cobamides and precursors that *C. difficile* can use *in vitro*, but which cobamides or cobamide precursors it predominantly uses in the gut remain to be discovered. Evidence from transcriptomics is ambiguous with respect to the expression of genes encoding cobamide-dependent enzymes or cobamide biosynthesis during infection, likely due to differences in study design (15, 43, 76–78). Since both diet and the microbiota can contribute to the cobamide profile in the gut (38, 79, 80), the availability of cobamides may vary significantly across infection systems and affect the expression and use of cobamide biosynthesis and cobamide-dependent pathways by *C. difficile*. In one study, *hemB*, which

**TABLE 1** Bacterial strains and plasmids

Strain or plasmid	Description	Source and/or reference
<b>Strains</b>		
<i>Escherichia coli</i> XL1-Blue		QB3 MacroLab
<i>Escherichia coli</i> CA434	<i>hsd20</i> (r <sub>B</sub> <sup>-</sup> m <sub>B</sub> <sup>-</sup> ) <i>recA13 rpsL20 leu proA2</i> ; with IncPb conjugative plasmid R702	Chain Biotech; 95
<i>Clostridioides difficile</i> 630 $\Delta$ erm	Erythromycin-sensitive strain	81
630 $\Delta$ erm $\Delta$ pyrE	Strain CRG1496	50
630 $\Delta$ erm $\Delta$ pyrE $\Delta$ btuFCD		This study
630 $\Delta$ erm $\Delta$ pyrE $\Delta$ cbiKJHGFTEDC		This study
630 $\Delta$ erm $\Delta$ pyrE $\Delta$ nrdDG		This study
<b>Plasmids</b>		
R702	Conjugation helper plasmid	95
pMTL-YN3	Allelic-exchange vector	50
pXL001	pMTL-YN3 containing the <i>btuFCD</i> deletion construct	This study
pXL002	pMTL-YN3 containing the <i>cbiKJHGFTEDC</i> deletion construct	This study
pXL003	pMTL-YN3 containing the <i>nrdDG</i> deletion construct	This study

encodes the enzyme that converts ALA to the next intermediate, porphobilinogen, was among the most highly expressed genes in *C. difficile* strain VPI 104363 in a mouse model (43), suggesting that *C. difficile* produces cobamides from ALA in the gut. How the cobamide content in the gut environment changes during *C. difficile* infection is unknown, but since much of the cobamide content in the lower gastrointestinal tract is produced by resident gut microbes (79, 80), it is possible that cobamide abundances change during dysbiosis. Further *in vivo* studies are needed to determine the extent to which cobamide metabolism is important for *C. difficile*-associated disease.

## MATERIALS AND METHODS

**Bacterial strains and growth conditions.** *C. difficile* 630  $\Delta$ erm, an erythromycin-sensitive derivative of the isolate 630 (81), and *C. difficile* 630  $\Delta$ erm  $\Delta$ pyrE, a derivative of 630  $\Delta$ erm with uracil auxotrophy (50), were streaked from frozen stocks onto brain heart infusion medium supplemented with 5 g/liter yeast extract and 0.1% L-cysteine (BHIS) agar (82) before being transferred to *Clostridium difficile* defined medium (CDDM) containing Casamino Acids (83) and 8 g/liter glucose. Agar plates and 96-well plates containing liquid cultures were incubated at 37°C in an anaerobic chamber (Coy Labs) containing 10% H<sub>2</sub>, 10% CO<sub>2</sub>, and 80% N<sub>2</sub>. For *C. difficile* 630  $\Delta$ erm  $\Delta$ pyrE and derived strains, 5  $\mu$ g/ml uracil was included in all defined media. For corrinoid extractions and NrdJ phenotype experiments, strains were cultured in CDDM plus 8 g/liter glucose. For MetH phenotype experiments, CDDMK plus 8 g/liter glucose without methionine was used. CDDMK contains the same salts, trace metals, and vitamins as CDDM, but the Casamino Acids, tryptophan, and cysteine are replaced with the following individual amino acids: 100 mg/liter histidine, 100 mg/liter tryptophan, 100 mg/liter glycine, 100 mg/liter tyrosine, 200 mg/liter arginine, 200 mg/liter phenylalanine, 200 mg/liter threonine, 200 mg/liter alanine, 300 mg/liter lysine, 300 mg/liter serine, 300 mg/liter valine, 300 mg/liter isoleucine, 300 mg/liter aspartic acid, 400 mg/liter leucine, 500 mg/liter cysteine, 600 mg/liter proline, and 900 mg/liter glutamic acid (40). All liquid defined media were prepared by boiling under 80% N<sub>2</sub>-20% CO<sub>2</sub> gas. After the pH stabilized between 6.8 and 7.2, the medium was dispensed into stoppered tubes and autoclaved. Filter-sterilized glucose and vitamins were added after autoclaving. Cultures in stoppered tubes were incubated at 37°C.

For MetH phenotype assays, *C. difficile* 630  $\Delta$ erm was grown in CDDM and then washed twice in CDDMK without methionine prior to inoculation in CDDMK at an optical density at 600 nm (OD<sub>600</sub>) of 0.01 in a 96-well plate. For NrdJ phenotype assays, *C. difficile* 630  $\Delta$ erm  $\Delta$ pyrE  $\Delta$ nrdDG was grown in CDDM with 5  $\mu$ g/ml uracil and 10 nM cyanocobalamin and washed three times in CDDM without cyanocobalamin prior to inoculation in CDDM at an OD<sub>600</sub> of 0.01 in a 96-well plate. The OD<sub>600</sub> was measured on a BioTek Synergy 2 plate reader after 22 to 24 h of growth.

ALA, Cbi, and cyanocobalamin were purchased from Sigma-Aldrich. Other cobamides were purified from bacterial cultures as described previously by Men et al. (84).

**Strain and plasmid construction.** The allele-coupled exchange (ACE) system described previously by Ng et al. was used for the construction of *C. difficile* mutant strains (50) (Table 1). Briefly, 500- to 1,000-bp sequences flanking the target gene(s) (arms of homology) in the *C. difficile* 630  $\Delta$ erm genome (GenBank accession number CP016318) were amplified by PCR (see Table S1 in the supplemental material) and then cloned into pMTL-YN3 (Chain Biotech) by Gibson assembly (85) in *Escherichia coli* XL1-Blue. Plasmid inserts were sequenced by Sanger sequencing before the transformation of the plasmid into *E. coli* CA434 (Chain Biotech). Conjugation of *E. coli* CA434 and *C. difficile* 630  $\Delta$ erm  $\Delta$ pyrE was performed as described previously (86), except that *C. difficile* and *E. coli* were each cultured for 5 to 8 h prior to pelleting *E. coli* and mixing with the *C. difficile* recipient. After 16 h of growth on BHIS agar,

the mixed cells were resuspended in 1 ml phosphate-buffered saline (PBS), and 100  $\mu$ l of the suspension was plated onto each of 5 to 7 plates of BHIS agar with 10  $\mu$ g/ml thiamphenicol, 250  $\mu$ g/ml D-cycloserine, and 16  $\mu$ g/ml ceftiofur added. Colonies were purified at least twice by streaking onto BHIS medium with 15  $\mu$ g/ml thiamphenicol, 250  $\mu$ g/ml D-cycloserine, and 16  $\mu$ g/ml ceftiofur, before counterselection on CDDM agar supplemented with 2 mg/liter 5-fluoroorotic acid (5-FOA) and 5  $\mu$ g/ml uracil. The resulting colonies were purified by streaking at least twice on counterselection medium prior to screening by colony PCR for the deletion and the presence of the *C. difficile* toxin gene *tcdB* (86). For the deletion of *nrdDG*, 10 nM cobalamin was added to all media during the ACE procedure.

**Corrinoid extraction and analysis.** *C. difficile* was grown in 50 ml CDDM plus 8 g/liter glucose under 80% N<sub>2</sub>–20% CO<sub>2</sub> headspace for 16 to 22 h at 37°C prior to corrinoid extraction. Two cultures were combined under each condition for a total volume of 100 ml for each extraction. Corrinoid extractions were performed as described previously (31), except that cell pellets were autoclaved for 35 min and cooled prior to the addition of methanol and potassium cyanide. Two or more biological replicates were performed under each condition.

High-performance liquid chromatography (HPLC) analysis was performed with an Agilent series 1200 system (Agilent Technologies, Santa Clara, CA) equipped with a diode array detector with detection wavelengths set at 360 and 525 nm. For Fig. 5B and Fig. 6A, samples were injected onto an Agilent Zorbax SB-Aq column (5  $\mu$ m; 4.6 by 150 mm) at 30°C, with a 1-ml/min flow rate. Compounds in the samples were separated with a gradient of 25 to 34% acidified methanol in acidified water (containing 0.1% formic acid) over 11 min, followed by a 34 to 50% gradient over 2 min and 50 to 75% over 9 min. For Fig. 5A, samples were injected onto an Agilent Eclipse Plus C<sub>18</sub> column (5  $\mu$ m; 9.4 by 250 mm) at 30°C, with a 2-ml/min flow rate. Compounds in the samples were separated with a gradient of 10 to 42% acidified methanol in acidified water over 20 min. The standards that were injected were as follows: Cbi (compound 1) at 200 pmol, pseudocobalamin (compound 2) at 225 pmol, cobalamin (compound 3) at 50 pmol, [Bza]Cba (compound 4) at 114 pmol, [2-MeAde]Cba (compound 5) at 114 pmol, and [Cre]Cba (compound 6) at 151 pmol. Five percent to 20% (by volume) *C. difficile* samples were injected.

***C. difficile* MLST tree construction.** For the 248 *C. difficile* genomes classified as “finished” or “permanent draft” in the JGI/IMG database (87) (<https://img.jgi.doe.gov/cgi-bin/mer/main.cgi> [accessed March 2019]), seven MLST gene sequences, *adh*, *atpA*, *dxr*, *glyA*, *recA*, *sodA*, and *tpi* (88), were downloaded and aligned individually using MUSCLE (89). The alignments were concatenated, and genomes missing one or more MLST genes or having duplicate genes were removed from the analysis, resulting in a total of 79 strains analyzed. The concatenated alignment was manually trimmed in UGENE (90), and columns with 95% or greater gaps were removed with trimAL (91). This alignment was used as the input for RAxML 8.2.12 (92) on the CIPRES Web server (<https://www.phylo.org/>) (93) with 100 bootstraps, using the GTRCAT model. The tree was visualized and annotated in iTOL (<https://itol.embl.de/>) (94).

## SUPPLEMENTAL MATERIAL

Supplemental material is available online only.

**SUPPLEMENTAL FILE 1**, PDF file, 0.2 MB.

## ACKNOWLEDGMENTS

This work was supported by NIH grants DP2AI117984 and R01GM114535 to M.E.T.

We thank Aimee Shen for her extensive advice and protocols for working with *C. difficile*, Craig Ellermeier for advice on working with *C. difficile*, and John Taylor, Gary Andersen, Christian Sieber, and Eric Dubinsky for advice on creating the phylogenetic tree. *C. difficile* 630  $\Delta$ *erm* and 630  $\Delta$ *erm*  $\Delta$ *pyrE* were provided to us by Andrew Hryckowian with permission from Nigel Minton. We thank Olga Sokolovskaya and Kenny Mok for help with HPLC analysis and Rita Nichiporuk at the QB3/Chemistry Mass Spectrometry Facility at UC Berkeley for performing the mass spectrometry analysis. We thank Luis Valentin-Alvarado for helpful discussions about *C. difficile* metabolism and genetic tools. We also thank Ellen Simms, Steve Lindow, Olga Sokolovskaya, Sebastian Gude, Gordon Pherribo, and Kenny Mok for critical reading of the manuscript.

A.N.S. performed growth experiments, corrinoid extractions, and phylogenetic analysis. X.L. and A.N.S. created the mutant strains. A.N.S. and M.E.T. wrote the manuscript.

## REFERENCES

- Lozupone CA, Stombaugh JI, Gordon JI, Jansson JK, Knight R. 2012. Diversity, stability and resilience of the human gut microbiota. *Nature* 489:220–230. <https://doi.org/10.1038/nature11550>.
- Magnúsdóttir S, Ravcheev D, De Crécy-Lagard V, Thiele I. 2015. Systematic genome assessment of B-vitamin biosynthesis suggests cooperation among gut microbes. *Front Genet* 6:148. <https://doi.org/10.3389/fgene.2015.00148>.
- D'Souza G, Waschina S, Pande S, Bohl K, Kaleta C, Kost C. 2014. Less is more: selective advantages can explain the prevalent loss of biosynthetic genes in bacteria. *Evolution* 68:2559–2570. <https://doi.org/10.1111/evo.12468>.
- Zengler K, Zaramela LS. 2018. The social network of microorganisms—how auxotrophies shape complex communities. *Nat Rev Microbiol* 16:383–390. <https://doi.org/10.1038/s41579-018-0004-5>.
- Garcia SL, Buck M, McMahon KD, Grossart HP, Eiler A, Warnecke F. 2015. Auxotrophy and intrapopulation complementarity in the ‘interactome’ of

- a cultivated freshwater model community. *Mol Ecol* 24:4449–4459. <https://doi.org/10.1111/mec.13319>.
6. Hubalek V, Buck M, Tan B, Foght J, Wendeberg A, Berry D, Bertilsson S, Eiler A. 2017. Vitamin and amino acid auxotrophy in anaerobic consortia operating under methanogenic conditions. *mSystems* 2:e00038-17. <https://doi.org/10.1128/mSystems.00038-17>.
  7. Belzer C, Chia LW, Aalvink S, Chamlagain B, Piironen V, Knol J, de Vos WM. 2017. Microbial metabolic networks at the mucus layer lead to diet-independent butyrate and vitamin B<sub>12</sub> production by intestinal symbionts. *mBio* 8:e00770-17. <https://doi.org/10.1128/mBio.00770-17>.
  8. Seth EC, Taga ME. 2014. Nutrient cross-feeding in the microbial world. *Front Microbiol* 5:350. <https://doi.org/10.3389/fmicb.2014.00350>.
  9. Lee WJ, Hase K. 2014. Gut microbiota-generated metabolites in animal health and disease. *Nat Chem Biol* 10:416–424. <https://doi.org/10.1038/nchembio.1535>.
  10. Lessa FC, Mu Y, Bamberg WM, Beldavs ZG, Dumyati GK, Dunn JR, Farley MM, Holzbauer SM, Meek JI, Phipps EC, Wilson LE, Winston LG, Cohen JA, Limbago BM, Fridkin SK, Gerding DN, McDonald LC. 2015. Burden of Clostridium difficile infection in the United States. *N Engl J Med* 372:825–834. <https://doi.org/10.1056/NEJMoa1408913>.
  11. Theriot CM, Koenigsnecht MJ, Carlson PE, Jr, Hatton GE, Nelson AM, Li B, Huffnagle GB, Li JZ, Young VB. 2014. Antibiotic-induced shifts in the mouse gut microbiome and metabolome increase susceptibility to Clostridium difficile infection. *Nat Commun* 5:3114. <https://doi.org/10.1038/ncomms4114>.
  12. Theriot CM, Young VB. 2014. Microbial and metabolic interactions between the gastrointestinal tract and Clostridium difficile infection. *Gut Microbes* 5:86–95. <https://doi.org/10.4161/gmic.27131>.
  13. Hryckowian AJ, Pruss KM, Sonnenburg JL. 2017. The emerging metabolic view of Clostridium difficile pathogenesis. *Curr Opin Microbiol* 35:42–47. <https://doi.org/10.1016/j.mib.2016.11.006>.
  14. Libertucci J, Young VB. 2019. The role of the microbiota in infectious diseases. *Nat Microbiol* 4:35–45. <https://doi.org/10.1038/s41564-018-0278-4>.
  15. Jenior ML, Leslie JL, Young VB, Schloss PD. 2017. Clostridium difficile colonizes alternative nutrient niches during infection across distinct murine gut microbiomes. *mSystems* 2:e00063-17. <https://doi.org/10.1128/mSystems.00063-17>.
  16. Jenior ML, Leslie JL, Young VB, Schloss PD. 2018. Clostridium difficile alters the structure and metabolism of distinct cecal microbiomes during initial infection to promote sustained colonization. *mSphere* 3:e00261-18. <https://doi.org/10.1128/mSphere.00261-18>.
  17. Carlucci C, Jones CS, Oliphant K, Yen S, Daigneault M, Carriero C, Robinson A, Petrof EO, Weese JS, Allen-Vercoe E. 2019. Effects of defined gut microbial ecosystem components on virulence determinants of Clostridioides difficile. *Sci Rep* 9:885. <https://doi.org/10.1038/s41598-018-37547-x>.
  18. Ferreyra JA, Wu KJ, Hryckowian AJ, Bouley DM, Weimer BC, Sonnenburg JL. 2014. Gut microbiota-produced succinate promotes C. difficile infection after antibiotic treatment or motility disturbance. *Cell Host Microbe* 16:770–777. <https://doi.org/10.1016/j.chom.2014.11.003>.
  19. Ng KM, Ferreyra JA, Higginbottom SK, Lynch JB, Kashyap PC, Gopinath S, Naidu N, Choudhury B, Weimer BC, Monack DM, Sonnenburg JL. 2013. Microbiota-liberated host sugars facilitate post-antibiotic expansion of enteric pathogens. *Nature* 502:96–99. <https://doi.org/10.1038/nature12503>.
  20. Darkoh C, Plants-Paris K, Bishoff D, DuPont HL. 2019. Clostridium difficile modulates the gut microbiota by inducing the production of indole, an interkingdom signaling and antimicrobial molecule. *mSystems* 4:e00346-18. <https://doi.org/10.1128/mSystems.00346-18>.
  21. Valdés-Varela L, Hernández-Barranco AM, Ruas-Madiedo P, Gueimonde M. 2016. Effect of Bifidobacterium upon Clostridium difficile growth and toxicity when co-cultured in different prebiotic substrates. *Front Microbiol* 7:738. <https://doi.org/10.3389/fmicb.2016.00738>.
  22. Buffie CG, Bucci V, Stein RR, McKenney PT, Ling L, Gobourne A, No D, Liu H, Kinnebrew M, Viale A, Littmann E, van den Brink MRM, Jenq RR, Taur Y, Sander C, Cross JR, Toussaint NC, Xavier JB, Pamer EG. 2015. Precision microbiome reconstitution restores bile acid mediated resistance to Clostridium difficile. *Nature* 517:205–208. <https://doi.org/10.1038/nature13828>.
  23. Kang JD, Myers CJ, Harris SC, Kakiyama G, Lee IK, Yun BS, Matsuzaki K, Furukawa M, Min HK, Bajaj JS, Zhou H, Hylemon PB. 2019. Bile acid 7 $\alpha$ -dehydroxylating gut bacteria secrete antibiotics that inhibit Clostridium difficile: role of secondary bile acids. *Cell Chem Biol* 26:27–34. <https://doi.org/10.1016/j.chembiol.2018.10.003>.
  24. Banerjee R, Ragsdale SW. 2003. The many faces of vitamin B12: catalysis by cobalamin-dependent enzymes. *Annu Rev Biochem* 72:209–247. <https://doi.org/10.1146/annurev.biochem.72.121801.161828>.
  25. Shelton AN, Seth EC, Mok KC, Han AW, Jackson SN, Haft DR, Taga ME. 2019. Uneven distribution of cobamide biosynthesis and dependence in bacteria predicted by comparative genomics. *ISME J* 13:789–804. <https://doi.org/10.1038/s41396-018-0304-9>.
  26. Rodionov DA, Vitreschak AG, Mironov AA, Gelfand MS. 2003. Comparative genomics of the vitamin B12 metabolism and regulation in prokaryotes. *J Biol Chem* 278:41148–41159. <https://doi.org/10.1074/jbc.M305837200>.
  27. Zhang Y, Rodionov DA, Gelfand MS, Gladyshev VN. 2009. Comparative genomics of nickel, cobalt and vitamin B12 utilization. *BMC Genomics* 10:78. <https://doi.org/10.1186/1471-2164-10-78>.
  28. Degnan PH, Barry NA, Mok KC, Taga ME, Goodman AL. 2014. Human gut microbes use multiple transporters to distinguish vitamin B12 analogs and compete in the gut. *Cell Host Microbe* 15:47–57. <https://doi.org/10.1016/j.chom.2013.12.007>.
  29. Rodionov DA, Arzamasov AA, Khoroshkin MS, Iablokov SN, Leyn SA, Peterson SN, Novichkov PS, Osterman AL. 2019. Micronutrient requirements and sharing capabilities of the human gut microbiome. *Front Microbiol* 10:1316. <https://doi.org/10.3389/fmicb.2019.01316>.
  30. Yan J, Ritalahti KM, Wagner DD, Löffler FE. 2012. Unexpected specificity of interspecies cobamide transfer from Geobacter spp. to organohalide-respiring Dehalococcoides mccartyi strains. *Appl Environ Microbiol* 78:6630–6636. <https://doi.org/10.1128/AEM.01535-12>.
  31. Yi S, Seth E, Men Y, Stabler SP, Allen RH, Alvarez-Cohen L, Taga ME. 2012. Versatility in corrinoid salvaging and remodeling pathways supports corrinoid-dependent metabolism in Dehalococcoides mccartyi. *Appl Environ Microbiol* 78:7745–7752. <https://doi.org/10.1128/AEM.02150-12>.
  32. Mok KC, Taga ME. 2013. Growth inhibition of Sporomusa ovata by incorporation of benzimidazole bases into cobamides. *J Bacteriol* 195:1902–1911. <https://doi.org/10.1128/JB.01282-12>.
  33. Helliwell KE, Lawrence AD, Holzer A, Kudahl UJ, Sasso S, Kräutler B, Scanlan DJ, Warren MJ, Smith AG. 2016. Cyanobacteria and eukaryotic algae use different chemical variants of vitamin B12. *Curr Biol* 26:999–1008. <https://doi.org/10.1016/j.cub.2016.02.041>.
  34. Yan J, Şimsir B, Farmer AT, Bi M, Yang Y, Campagna SR, Löffler FE. 2016. The corrinoid cofactor of reductive dehalogenases affects dechlorination rates and extents in organohalide-respiring Dehalococcoides mccartyi. *ISME J* 10:1092–1101. <https://doi.org/10.1038/ismej.2015.197>.
  35. Keller S, Kunze C, Bommer M, Paetz C, Menezes RC, Dobbek H, Schubert T. 2018. Selective utilization of benzimidazolyl-norcobamides as cofactors by the tetrachloroethene reductive dehalogenase of Sulfurospirillum multivorans. *J Bacteriol* 200:e00584-17. <https://doi.org/10.1128/JB.00584-17>.
  36. Crofts TS, Seth EC, Hazra AB, Taga ME. 2013. Cobamide structure depends on both lower ligand availability and CobT substrate specificity. *Chem Biol* 20:1265–1274. <https://doi.org/10.1016/j.chembiol.2013.08.006>.
  37. Sokolovskaya OM, Mok KC, Park JD, Tran JLA, Quanstrom KA, Taga ME. 2019. Cofactor selectivity in methylmalonyl coenzyme A mutase, a model cobamide-dependent enzyme. *mBio* 10:e01303-19. <https://doi.org/10.1128/mBio.01303-19>.
  38. Allen RH, Stabler SP. 2008. Identification and quantitation of cobalamin and cobalamin analogues in human feces. *Am J Clin Nutr* 87:1324–1335. <https://doi.org/10.1093/ajcn/87.5.1324>.
  39. Abreu NA, Taga ME. 2016. Decoding molecular interactions in microbial communities. *FEMS Microbiol Rev* 40:648–663. <https://doi.org/10.1093/femsre/fuw019>.
  40. Karasawa T, Ikoma S, Yamakawa K, Nakamura S. 1995. A defined growth medium for Clostridium difficile. *Microbiology* 141:371–375. <https://doi.org/10.1099/13500872-141-2-371>.
  41. Nawrocki KL, Wetzell D, Jones JB, Woods EC, McBride SM. 2018. Ethanolamine is a valuable nutrient source that impacts Clostridium difficile pathogenesis. *Environ Microbiol* 20:1419–1435. <https://doi.org/10.1111/1462-2920.14048>.
  42. Dannheim H, Will SE, Schomburg D, Neumann-Schaal M. 2017. Clostridioides difficile 630 $\Delta$ erm in silico and in vivo—quantitative growth and extensive polysaccharide secretion. *FEBS Open Bio* 7:602–615. <https://doi.org/10.1002/2211-5463.12208>.
  43. Fletcher JR, Erwin S, Lanzas C, Theriot CM. 2018. Shifts in the gut metabolome and Clostridium difficile transcriptome throughout colonization and infection in a mouse model. *mSphere* 3:e00089-18. <https://doi.org/10.1128/mSphere.00089-18>.

44. Köpke M, Straub M, Dürre P. 2013. *Clostridium difficile* is an autotrophic bacterial pathogen. *PLoS One* 8:e62157. <https://doi.org/10.1371/journal.pone.0062157>.
45. Avissar YJ, Beale SI. 1989. Identification of the enzymatic basis for  $\Delta$ -aminolevulinic acid auxotrophy in a hemA mutant of *Escherichia coli*. *J Bacteriol* 171:2919–2924. <https://doi.org/10.1128/jb.171.6.2919-2924.1989>.
46. Roth JR, Lawrence JG, Bobik TA. 1996. Cobalamin (coenzyme B12): synthesis and biological significance. *Annu Rev Microbiol* 50:137–181. <https://doi.org/10.1146/annurev.micro.50.1.137>.
47. Haslam SC, Ketley JM, Mitchell TJ, Stephen J, Burdon DW, Candy DC. 1986. Growth of *Clostridium difficile* and production of toxins A and B in complex and defined media. *J Med Microbiol* 21:293–297. <https://doi.org/10.1099/00222615-21-4-293>.
48. Anderson PJ, Lango J, Carkeet C, Britten A, Kräutler B, Hammock BD, Roth JR. 2008. One pathway can incorporate either adenine or dimethylbenzimidazole as an  $\alpha$ -axial ligand of B12 cofactors in *Salmonella enterica*. *J Bacteriol* 190:1160–1171. <https://doi.org/10.1128/JB.01386-07>.
49. Chan CH, Escalante-Semerena JC. 2011. ArsAB, a novel enzyme from *Sporosarcina ovata* activates phenolic bases for adenosylcobamide biosynthesis. *Mol Microbiol* 81:952–967. <https://doi.org/10.1111/j.1365-2958.2011.07741.x>.
50. Ng YK, Ehsaan M, Philip S, Coltery MM, Janoir C, Collignon A, Cartman ST, Minton NP. 2013. Expanding the repertoire of gene tools for precise manipulation of the *Clostridium difficile* genome: allelic exchange using pyrE alleles. *PLoS One* 8:e56051. <https://doi.org/10.1371/journal.pone.0056051>.
51. Barker HA. 1967. Biochemical functions of corrinoid compounds: the sixth Hopkins Memorial Lecture. *Biochem J* 105:1–15. <https://doi.org/10.1042/bj1050001>.
52. Watanabe F, Nakano Y, Stupperich E. 1992. Different corrinoid specificities for cell growth and the cobalamin uptake system in *Euglena gracilis* z. *J Gen Microbiol* 138:1807–1813. <https://doi.org/10.1099/00221287-138-9-1807>.
53. Campbell GRO, Taga ME, Mistry K, Lloret J, Anderson PJ, Roth JR, Walker GC. 2006. Sinorhizobium meliloti bluB is necessary for production of 5,6-dimethylbenzimidazole, the lower ligand of B12. *Proc Natl Acad Sci U S A* 103:4634–4639. <https://doi.org/10.1073/pnas.0509384103>.
54. Taga ME, Larsen NA, Howard-Jones AR, Walsh CT, Walker GC. 2007. BluB cannibalizes flavin to form the lower ligand of vitamin B12. *Nature* 446:449–453. <https://doi.org/10.1038/nature05611>.
55. Gray MJ, Escalante-Semerena JC. 2007. Single-enzyme conversion of FMNH<sub>2</sub> to 5,6-dimethylbenzimidazole, the lower ligand of B12. *Proc Natl Acad Sci U S A* 104:2921–2926. <https://doi.org/10.1073/pnas.0609270104>.
56. Hazra AB, Tran JLA, Crofts TS, Taga ME. 2013. Analysis of substrate specificity in CobT homologs reveals widespread preference for DMB, the lower axial ligand of vitamin B12. *Chem Biol* 20:1275–1285. <https://doi.org/10.1016/j.chembiol.2013.08.007>.
57. Crofts TS, Hazra AB, Tran JLA, Sokolovskaya OM, Osadchiv V, Ad O, Pelton J, Bauer S, Taga ME. 2014. Regiospecific formation of cobamide isomers is directed by CobT. *Biochemistry* 53:7805–7815. <https://doi.org/10.1021/bi501147d>.
58. Hazra AB, Han AW, Mehta AP, Mok KC, Osadchiv V, Begley TP, Taga ME. 2015. Anaerobic biosynthesis of the lower ligand of vitamin B12. *Proc Natl Acad Sci U S A* 112:10792–10797. <https://doi.org/10.1073/pnas.1509132112>.
59. Yan J, Bi M, Bourdon AK, Farmer AT, Wang PH, Molenda O, Quaille AT, Jiang N, Yang Y, Yin Y, Şimşir B, Campagna SR, Edwards EA, Löffler FE. 2018. Purinyl-cobamide is a native prosthetic group of reductive dehalogenases. *Nat Chem Biol* 14:8–14. <https://doi.org/10.1038/nchembio.2512>.
60. Keller S, Ruetz M, Kunze C, Kräutler B, Diekert G, Schubert T. 2014. Exogenous 5,6-dimethylbenzimidazole caused production of a non-functional tetrachloroethene reductive dehalogenase in *Sulfurospirillum multivorans*. *Environ Microbiol* 16:3361–3369. <https://doi.org/10.1111/1462-2920.12268>.
61. Yan J, Im J, Yang Y, Löffler FE. 2013. Guided cobalamin biosynthesis supports *Dehalococcoides mccartyi* reductive dechlorination activity. *Philos Trans R Soc Lond B Biol Sci* 368:20120320. <https://doi.org/10.1098/rstb.2012.0320>.
62. Woodson JD, Escalante-Semerena JC. 2004. CbiZ, an amidohydrolase enzyme required for salvaging the coenzyme B12 precursor cobinamide in archaea. *Proc Natl Acad Sci U S A* 101:3591–3596. <https://doi.org/10.1073/pnas.0305939101>.
63. Gray MJ, Escalante-Semerena JC. 2009. The cobinamide amidohydrolase (cobyric acid-forming) CbiZ enzyme: a critical activity of the cobamide remodelling system of *Rhodobacter sphaeroides*. *Mol Microbiol* 74:1198–1210. <https://doi.org/10.1111/j.1365-2958.2009.06928.x>.
64. Gray MJ, Escalante-Semerena JC. 2009. In vivo analysis of cobinamide salvaging in *Rhodobacter sphaeroides* strain 2.4.1. *J Bacteriol* 191:3842–3851. <https://doi.org/10.1128/JB.00230-09>.
65. Borths EL, Locher KP, Lee AT, Rees DC. 2002. The structure of *Escherichia coli* BtuF and binding to its cognate ATP binding cassette transporter. *Proc Natl Acad Sci U S A* 99:16642–16647. <https://doi.org/10.1073/pnas.262659699>.
66. Mireku SA, Ruetz M, Zhou T, Korkhov VM, Kräutler B, Locher KP. 2017. Conformational change of a tryptophan residue in BtuF facilitates binding and transport of cobinamide by the vitamin B12 transporter BtuCD-F. *Sci Rep* 7:41575. <https://doi.org/10.1038/srep41575>.
67. Vitreschak AG, Rodionov DA, Mironov AA, Gelfand MS. 2003. Regulation of the vitamin B12 metabolism and transport in bacteria by a conserved RNA structural element. *RNA* 9:1084–1097. <https://doi.org/10.1261/rna.5710303>.
68. Nahvi A, Sudarsan N, Ebert MS, Zou X, Brown KL, Breaker RR. 2002. Genetic control by a metabolite binding mRNA. *Chem Biol* 9:1043–1049. [https://doi.org/10.1016/s1074-5521\(02\)00224-7](https://doi.org/10.1016/s1074-5521(02)00224-7).
69. Nahvi A, Barrick JE, Breaker RR. 2004. Coenzyme B12 riboswitches are widespread genetic control elements in prokaryotes. *Nucleic Acids Res* 32:143–150. <https://doi.org/10.1093/nar/gkh167>.
70. Perez AA, Rodionov DA, Bryant DA. 2016. Identification and regulation of genes for cobalamin transport in the cyanobacterium *Synechococcus* sp. strain PCC 7002. *J Bacteriol* 198:2753–2761. <https://doi.org/10.1128/JB.00476-16>.
71. Stabler RA, Rose G, Gerding DN, Lawley TD, Quail MA, Wren BW, Gibert M, Dawson L, Parkhill J, Sebahia M, Dougan G, Valiente E, Corton C, Martin M, Popoff MR, He M. 2009. Comparative genome and phenotypic analysis of *Clostridium difficile* O27 strains provides insight into the evolution of a hypervirulent bacterium. *Genome Biol* 10:R102. <https://doi.org/10.1186/gb-2009-10-9-r102>.
72. Tanioka Y, Miyamoto E, Yabuta Y, Ohnishi K, Fujita T, Yamaji R, Misono H, Shigeoka S, Nakano Y, Inui H, Watanabe F. 2010. Methyladeninylcobamide functions as the cofactor of methionine synthase in a cyanobacterium, *Spirulina platensis* NIES-39. *FEBS Lett* 584:3223–3226. <https://doi.org/10.1016/j.febslet.2010.06.013>.
73. Taga ME, Walker GC. 2010. Sinorhizobium meliloti requires a cobalamin-dependent ribonucleotide reductase for symbiosis with its plant host. *Mol Plant Microbe Interact* 23:1643–1654. <https://doi.org/10.1094/MPMI-07-10-0151>.
74. Cadieux N, Bradbeer C, Reeger-Schneider E, Köster W, Mohanty AK, Wiener MC, Kadner RJ. 2002. Identification of the periplasmic cobalamin-binding protein BtuF of *Escherichia coli*. *J Bacteriol* 184:706–717. <https://doi.org/10.1128/jb.184.3.706-717.2002>.
75. Crofts TS, Men Y, Alvarez-Cohen L, Taga ME. 2014. A bioassay for the detection of benzimidazoles reveals their presence in a range of environmental samples. *Front Microbiol* 5:592. <https://doi.org/10.3389/fmicb.2014.00592>.
76. Janoir C, Denève C, Bouttier S, Barbut F, Hoys S, Caleechum L, Chapetón-Montes D, Pereira FC, Henriques AO, Collignon A, Monot M, Dupuy B. 2013. Adaptive strategies and pathogenesis of *Clostridium difficile* from in vivo transcriptomics. *Infect Immun* 81:3757–3769. <https://doi.org/10.1128/IAI.00515-13>.
77. Kansau I, Barketi-Klai A, Monot M, Hoys S, Dupuy B, Janoir C, Collignon A. 2016. Deciphering adaptation strategies of the epidemic *Clostridium difficile* O27 strain during infection through in vivo transcriptional analysis. *PLoS One* 11:e0158204. <https://doi.org/10.1371/journal.pone.0158204>.
78. Scaria J, Janvilisri T, Fubini S, Gleed RD, McDonough SP, Chang YF. 2011. *Clostridium difficile* transcriptome analysis using pig ligated loop model reveals modulation of pathways not modulated in vitro. *J Infect Dis* 203:1613–1620. <https://doi.org/10.1093/infdis/jir112>.
79. Herbert V. 1988. Vitamin B12: plant sources, requirements, and assay. *Am J Clin Nutr* 48:852–858. <https://doi.org/10.1093/ajcn/48.3.852>.
80. Degnan PH, Taga ME, Goodman AL. 2014. Vitamin B12 as a modulator of gut microbial ecology. *Cell Metab* 20:769–778. <https://doi.org/10.1016/j.cmet.2014.10.002>.
81. Hussain HA, Roberts AP, Mullany P. 2005. Generation of an erythromycin-sensitive derivative of *Clostridium difficile* strain 630

- (630Δerm) and demonstration that the conjugative transposon Tn916ΔE enters the genome of this strain at multiple sites. *J Med Microbiol* 54:137–141. <https://doi.org/10.1099/jmm.0.45790-0>.
82. Sorg JA, Dineen SS. 2009. Laboratory maintenance of *Clostridium difficile*. *Curr Protoc Microbiol* Chapter 9:Unit 9A.1. <https://doi.org/10.1002/9780471729259.mc09a01s12>.
83. Cartman ST, Minton NP. 2010. A mariner-based transposon system for in vivo random mutagenesis of *Clostridium difficile*. *Appl Environ Microbiol* 76:1103–1109. <https://doi.org/10.1128/AEM.02525-09>.
84. Men Y, Seth EC, Yi S, Allen RH, Taga ME, Alvarez-Cohen L. 2014. Sustainable growth of *Dehalococcoides mccartyi* 195 by corrinoid salvaging and remodeling in defined lactate-fermenting consortia. *Appl Environ Microbiol* 80:2133–2141. <https://doi.org/10.1128/AEM.03477-13>.
85. Gibson DG, Young L, Chuang RY, Venter JC, Hutchison CA, Smith HO. 2009. Enzymatic assembly of DNA molecules up to several hundred kilobases. *Nat Methods* 6:343–345. <https://doi.org/10.1038/nmeth.1318>.
86. Bouillaut L, McBride SM, Sorg JA. 2011. Genetic manipulation of *Clostridium difficile*. *Curr Protoc Microbiol* Chapter 9:Unit 9A.2. <https://doi.org/10.1002/9780471729259.mc09a02s20>.
87. Chen IMA, Chu K, Palaniappan K, Pillay M, Ratner A, Huang J, Huntemann M, Varghese N, White JR, Seshadri R, Smirnova T, Kirton E, Jungbluth SP, Woyke T, Eloie-Fadrosch EA, Ivanova NN, Kyrpides NC. 2019. IMG/M v.5.0: an integrated data management and comparative analysis system for microbial genomes and microbiomes. *Nucleic Acids Res* 47:D666–D677. <https://doi.org/10.1093/nar/gky901>.
88. Griffiths D, Fawley W, Kachrimanidou M, Bowden R, Crook DW, Fung R, Golubchik T, Harding RM, Jeffery KJM, Jolley KA, Kirton R, Peto TE, Rees G, Stoesser N, Vaughan A, Walker AS, Young BC, Wilcox M, Dingle KE. 2010. Multilocus sequence typing of *Clostridium difficile*. *J Clin Microbiol* 48:770–778. <https://doi.org/10.1128/JCM.01796-09>.
89. Edgar RC. 2004. MUSCLE: multiple sequence alignment with high accuracy and high throughput. *Nucleic Acids Res* 32:1792–1797. <https://doi.org/10.1093/nar/gkh340>.
90. Okonechnikov K, Golosova O, Fursov M, UGENE Team. 2012. Unipro UGENE: a unified bioinformatics toolkit. *Bioinformatics* 28:1166–1167. <https://doi.org/10.1093/bioinformatics/bts091>.
91. Capella-Gutiérrez S, Silla-Martínez JM, Gabaldón T. 2009. trimAl: a tool for automated alignment trimming in large-scale phylogenetic analyses. *Bioinformatics* 25:1972–1973. <https://doi.org/10.1093/bioinformatics/btp348>.
92. Stamatakis A. 2014. RAxML version 8: a tool for phylogenetic analysis and post-analysis of large phylogenies. *Bioinformatics* 30:1312–1313. <https://doi.org/10.1093/bioinformatics/btu033>.
93. Miller MA, Pfeiffer W, Schwartz T. 2010. Creating the CIPRES Science Gateway for inference of large phylogenetic trees. *Abstr 2010 Gateway Comput Environ Workshop*.
94. Letunic I, Bork P. 2016. Interactive tree of life (iTOL) v3: an online tool for the display and annotation of phylogenetic and other trees. *Nucleic Acids Res* 44:W242–W245. <https://doi.org/10.1093/nar/gkw290>.
95. Williams DR, Young DI, Young M. 1990. Conjugative plasmid transfer from *Escherichia coli* to *Clostridium acetobutylicum*. *J Gen Microbiol* 136:819–826. <https://doi.org/10.1099/00221287-136-5-819>.